NASA Technical Memorandum 78968

(NASA-TM-78968) VELOCITY, TEMPERATURE, AND ELECTRICAL CONDUCTIVITY PROFILES IN HYDROGEN-OXYGEN MHD DUCT FLOWS (NASA) 11 p HC A02/MF A01 CSCL 20D

N78-28372

Unclas
G3/34 27107

VELOCITY, TEMPERATURE, AND ELECTRICAL CONDUCTIVITY PROFILES IN HYDROGEN-OXYGEN MHD DUCT FLOWS

Mahesh S. Greywall
Wichita State University
Wichita, Kansas 67108

and

Carlson C. P. Pian
Lewis Research Center
Cleveland, Ohio 44135

TECHNICAL PAPER to be presented at the
Winter Annual Meeting
sponsored by American Society of Mechanical Engineers
San Francisco, California, December 10-15, 1978

VELOCITY, TEMPERATURE, AND ELECTRICAL CONDUCTIVITY PROFILES IN HYDROGEN-OXYGEN MHD DUCT FLOWS*

Mahesh S. Greywall
Department of Mechanical Engineering
Wichita State University
Wichita, Kansas 67108

Carlson C. P. Pian
NASA Lewis Research Center
Cleveland, Ohio 44135

ABSTRACT

This paper presents results of two-dimensional duct flow computations for radial distributions of velocity, temperature, and electrical conductivity. Calculations were carried out for the flow conditions representative of NASA Lewis hydrogen-oxygen combustion driven MHD duct. Results are presented for two sets of computations: (1) profiles of developing flow in a smooth duct, and (2) profiles of fully developed pipe flow with a specified streamwise shear stress distribution. The predicted temperature and electrical conductivity profiles for the developing flows compared well with available experimental data.

I. INTRODUCTION

Magnetohydrodynamic (MHD) power generation utilizes the interaction of an electrically conducting gas flowing through a duct with an externally applied magnetic field to convert a portion of the energy of the gas directly into electricity. An accurate estimation of the fluid's electrical conductivity (σ) during its passage through the MHD duct is crucial to one's ability to predict the generator performance. Smith (ref. 1) performed a series of tests to measure the electrical properties of a cesium seeded H_2-O_2 combustion gas. The results of the bulk electrical conductivity measurements were found to be in good agreement with the one-dimensional calculations of reference 1. To gain insight into the radial distribution of the electrical conductivity and flow properties, Wang and Smith (ref. 2) made spectroscopic measurements of transverse profiles of the absolute integrated intensity from the optically thin lines of cesium atoms. The radial profiles of the cesium emission coefficients were then obtained by Abel inversion. These emission coefficients were used to infer the radial temperature distributions for cases where the density of the cesium atoms can be assumed uniform across the duct. Alternatively, the radial σ and seed density distributions can also be inferred from the emission coefficients by using temperature profiles estimated from theoretical considerations (ref. 2).

* Work partially funded under Department of Energy Interagency Agreement No. EF-77-A-01-2647 and also under NASA Grant NSG-3186.

To add to the theoretical background for the understanding of these flows, a two-dimensional calculation of these flows was undertaken. This paper presents the results of preliminary computations for the radial distributions of velocity, temperature, and electrical conductivity for the duct geometry and flow conditions typical of the experiments of references 1 and 2: stoichiometric H_2-O_2 combustion gas seeded with cesium hydroxide flowing through a constant area duct (2.53 cm radius) with centerline velocity and temperature of the order of 2500 m/s and 3000 K respectively, heat sink wall temperature of approximately 600K, and burner pressure of 1100 kPa (10.9 atm).

Two different sets of computations were carried out. In the first set of calculations the initial profiles at the beginning of the duct are varied to simulate different amounts of boundary layer blockage until the resulting temperature profile gave the best fit to the experimental data. Also in these computations, the axial pressure variation was calculated as part of the confined flow solutions. In the second set of computations, the temperature and velocity profiles were calculated assuming the limiting case that the flow is fully developed. Also in the latter set, the shear stress at the wall was adjusted to yield the experimentally observed axial pressure variation.

In all the calculations, the thermodynamic and transport properties of the gas mixture were calculated assuming local thermodynamic equilibrium following Gordon and McBride (ref. 3) and Svehla and McBride (ref. 4). The electrical conductivity of the gas was calculated as in Smith and Nichols (ref. 5).

II. DEVELOPING FLOW SOLUTIONS

The partially developed entrance flow in a MHD duct was analyzed in the first set of calculations. The streamwise pressure variations are calculated as part of the confined flow solutions. The numerical scheme of Patankar and Spalding (ref. 6) was used. Modifications were added to handle the variable fluid properties and to calculate the streamwise pressure variation using a predictor-corrector scheme. For greater details, the reader is referred to the work in reference 7.

The experimental duct of references 1 and 2 was connected to an expansion nozzle. The flow consequently entered the duct with the boundary layer already partially developed. The exact amount of this development is not known. Hence the following procedure was followed in the specification of the initial dependent variable profiles at the duct entrance. A two-layer profile is used for the velocity distribution (see Figure 1). In the centerline region, a uniform velocity, $u_{\mathbb{C}}$, has been assumed. A 1/7-power-velocity distribution law is used near the wall. The total enthalpy distribution is assumed to be similar to that of the velocity. The value of R_1 at the channel entrance is varied to account for the unknown degree of initial boundary layer development. The values of the centerline velocity and total enthalpy must still be determined for a given value of R_1. This is accomplished by matching the gross flow features (mass and enthalpy fluxes, implicit in the assumed initial profiles) to those flow conditions at the combustor/nozzle exit. The rocket option of reference 3 is used to calculate the total enthalpy flux out of the combustor/nozzle for the given hydrogen-oxygen ratio, seed fraction (SF), combustor pressure (P_C), isentropic expansion ratio, and combustor efficiency. An initial guess is made for the values of the centerline velocity and total enthalpy in the initial profiles. From these, mass and total enthalpy fluxes can be calculated and compared to those values at the combustor/nozzle exit. The guessed values are then adjusted and the process is repeated. This iterative procedure is continued until the assumed centerline values yields mass and enthalpy fluxes that agree with the known upstream nozzle exit conditions.

Figure 2 shows the calculated temperature profiles at .09 meters downstream of the duct inlet for three values of seed fraction. The axial location corresponded to the measurement station in reference 2. In these calculations the chamber pressure equaled 1100 kPa, wall temperature equaled 600K, and the amount of combustor heat loss was taken to be 6% of the total thermal input. It can be seen that there is a slight drop in the predicted centerline temperatures when the values of SF are increased. This trend is as expected. The alkali-metal seed is injected into the combustion chamber in the form of CsOH dissolved in water. As the seed fraction is increased, this diluent will decrease the flame temperature and consequently the gas temperature.

For comparison, the measured temperature profiles at the corresponding seed fractions are also plotted in Figure 2. There are some run-to-run deviations in the experimental data and the results shown are from typical runs. The agreement in the profile shapes between the developing flow results and the measured data is due to an adjustment of the amount of boundary layer development in the unknown initial profiles, as discussed earlier. There is a general tendency to overpredict the gas temperature in the near wall region. There are several possible explanations for these near wall discrepancies. One of the most probable causes may have originated from the optical viewports which were cut in the test section walls. These ports may have provoked localized three-dimensional flow disturbances such as recirculations, flow detachments and/or wakes. The relatively cold nitrogen gas used to purge the quartz windows may have also worked its way to the duct wall region to lower the gas temperature there.

The computed and measured electrical conductivity distributions for three values of SF's are shown in Figure 3. The conductivity deteriorated badly in the outer portion of the channel due to the rather thick thermal boundary layers associated with the heat sink walls.

III. FULLY DEVELOPED FLOW CALCULATIONS

The second set of calculations were carried out using a newly developed numerical technique to compute two-dimensional duct flows. The details are given in reference 8. Basically the technique is as follows: The total flow in the duct is partitioned into a sequence of finite streams. The difference equations to calculate the flow properties are then obtained by applying the conservation principles directly to the individual streams.

The results presented in this section are for fully developed flows. Computations were carried out along the duct until the axial variations of the velocity and temperature radial profiles became negligible. To save computational time, the initial profiles at the beginning of the duct were mocked up, guided by the results of numerical experimentation, to produce fully developed profiles in about two pipe diameters (approximately 10 cm) from the starting point.

Due to the nature of the experimental duct, some features of the flow are difficult to account for during numerical simulation. For example, weak oblique shock waves were detected in the duct during the experiments of reference 1. Some of these disturbances originated from the rocket-type nozzle which was designed to achieve low weight rather than perfectly parallel flow at the nozzle exit. Pressure disturbances can also arise from the optical viewports and other "roughness" on the duct walls. Not only is this complex flow phenomena of shock-boundary layer interaction beyond the scope of our present two-dimensional computational methods, but also the presence of these weak pressure disturbances confuse the issue as to what fraction of the pressure rise experimentally observed along the supersonic duct is actually due to friction at the wall. In this set of calculations, the pressure rise along the duct was taken as a specified parameter. During the computations the shear stress at the wall (i.e., surface roughness) was iterated upon until the calculated pressure gradient equaled the specified distribution. Figure 4 shows the experimental data of reference 1 for the streamwise pressure variation. To bracket the data, two pressure gradient lines were drawn as shown. Thus the calculations were carried out for the specified pressure gradients of 280 and 180 kPa/m. The seed fraction equaled 5%.

Results of the computations are shown in Figure 5. This figure shows the radial distributions of velocity and temperature for the two values of dp/dx considered. The shear stress at the wall for 280 kPa/m pressure rise was 1.8 kPa and that for 180 kPa/m was 1.3 kPa. From the velocity distribution curves we note a slight flattening of the profiles with lower pressure gradient. This is in accord with what will be expected with lower wall stress (lower wall roughness) that goes with the lower pressure gradient. The temperature profiles for the two cases were found to be very close. The difference was too small to be shown in the figure thus both cases are shown as a single curve.

In Figure 6 we have compared the results for radial temperature distribution as calculated in section II and section III with the experimental data. From this figure we note that the flow 9 cms downstream of the beginning of the channel, where the measurements were made, is still developing.

IV. SUMMARY

Two-dimensional analyses of the NASA Lewis cesium-seeded H_2-O_2 MHD duct flow have been performed. The results of two sets of computations are presented: (1) profiles of the developing flow in a smooth duct, and (2) profiles of fully developed pipe flow with specified streamwise shear stress distribution. The predicted temperature and electrical conductivity profiles for the developing flows compared well with the experimental results, although some slight discrepancies were observed. The possible sources of these discrepancies are noted.

REFERENCES

1. Smith, J. M., "Results and Progress on the NASA Lewis H_2-O_2 MHD Program," Presented at the 15th Symposium on the Engineering Aspects of Magnetohydrodynamics, The University of Pennsylvania, Philadelphia, PA, May 24-16, 1976.

2. Wang, S. Y. and Smith, J. M., "Spectroscopic Determination of Electrical Conductivity in an MHD Duct from Absolute Intensity Measurements," Proceedings 16th Symposium on the Engineering Aspects of Magnetohydrodynamics, Energy Research and Development Administration, pp. V.1.1-V.1.5, 1977.

3. Gordon, S. and McBride, B. J., "Computer Program for Calculation of Complex Chemical Equilibrium Compositions, Rocket Performance, Incident and Reflected Shocks, and Chapman-Jouquet Detonations," NASA SP-273, 1967.

4. Svehla, R. A. and McBride, B. J., "FORTRAN IV Computer Program for Calculations of Thermodynamic and Transport Properties of Complex Chemical Systems," NASA TN D-7056, 1973.

5. Smith, J.M. and Nichols, L. D., "Estimation of Optimal Operating Conditions for Hydrogen-Oxygen Cesium Seeded Magnetohydrodynamic Power Generator," NASA TN D-8374, 1977.

6. Patankar, S. V. and Spalding, D. B., Heat and Mass Transfer in Boundary Layers, 2nd ed., Intertext Books, London, 1970.

7. Pian, C. C. P. and Wang, S. Y., "Estimation of the Electrical Conductivity in a Cesium Seeded Hydrogen-Oxygen Magnetohydrodynamic Generator Duct," Proposed NASA Technical Paper, 1978.

8. Greywall, M. S., "Two Dimensional Duct Flow Code," ME-GL-78-1, Department of Mechanical Engineering, Wichita State University, Wichita, Kansas.

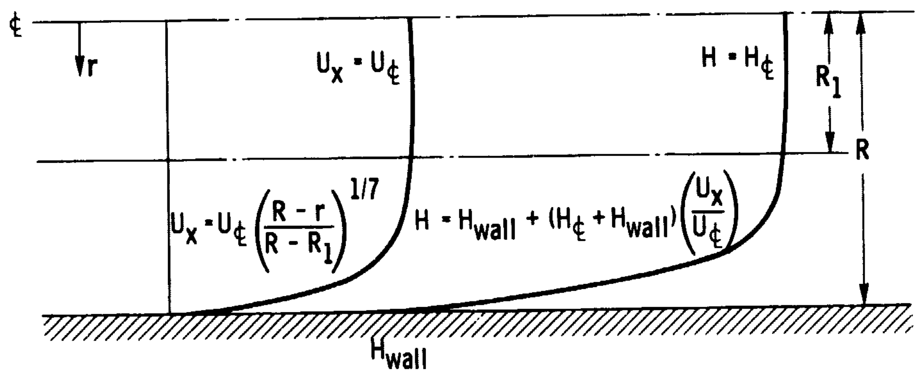

Figure 1. - Initial velocity and total enthalpy profiles used in the developing flow calculations.

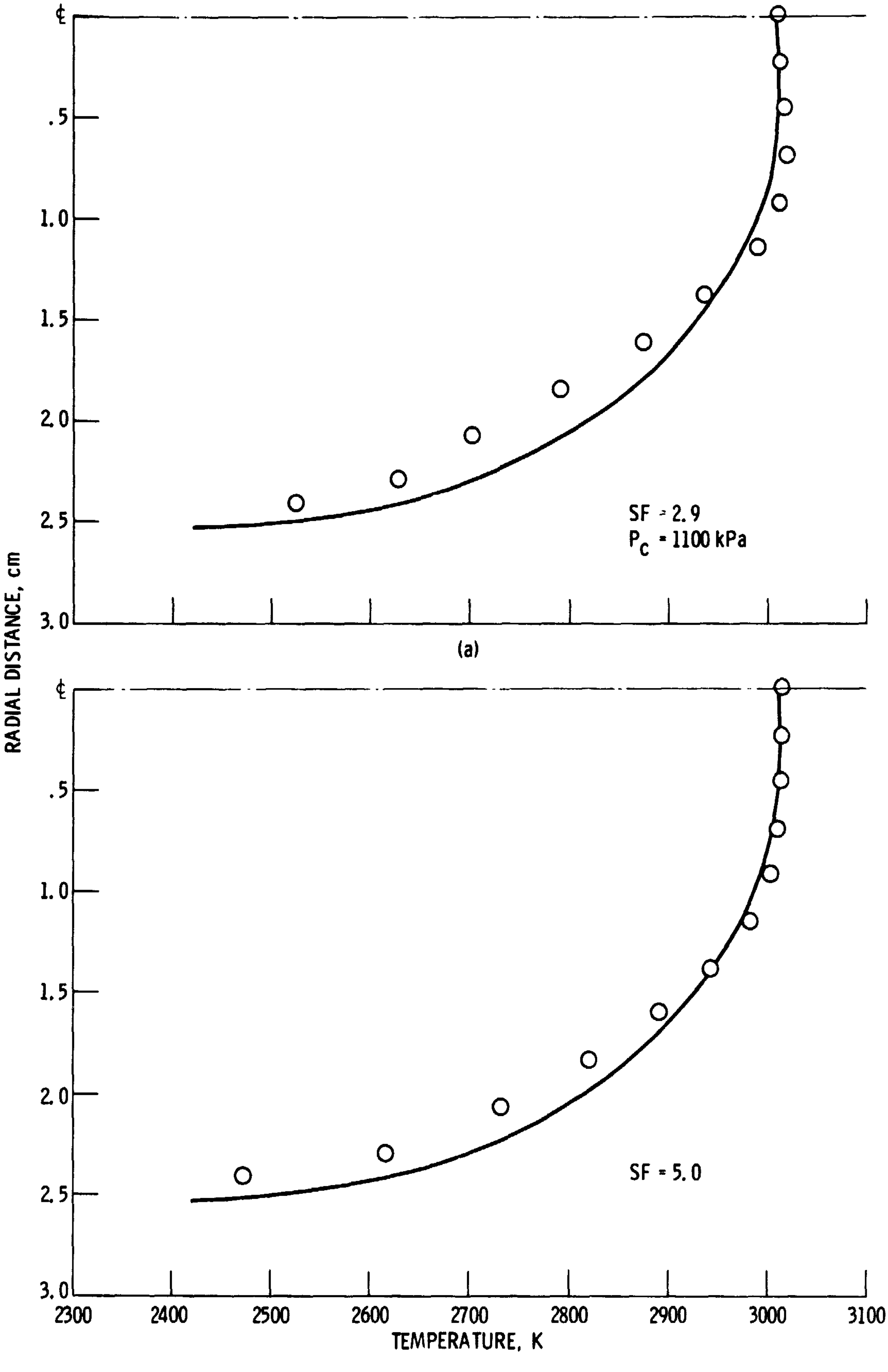

Figure 2. - Comparison with data for turbulent temperature profiles.

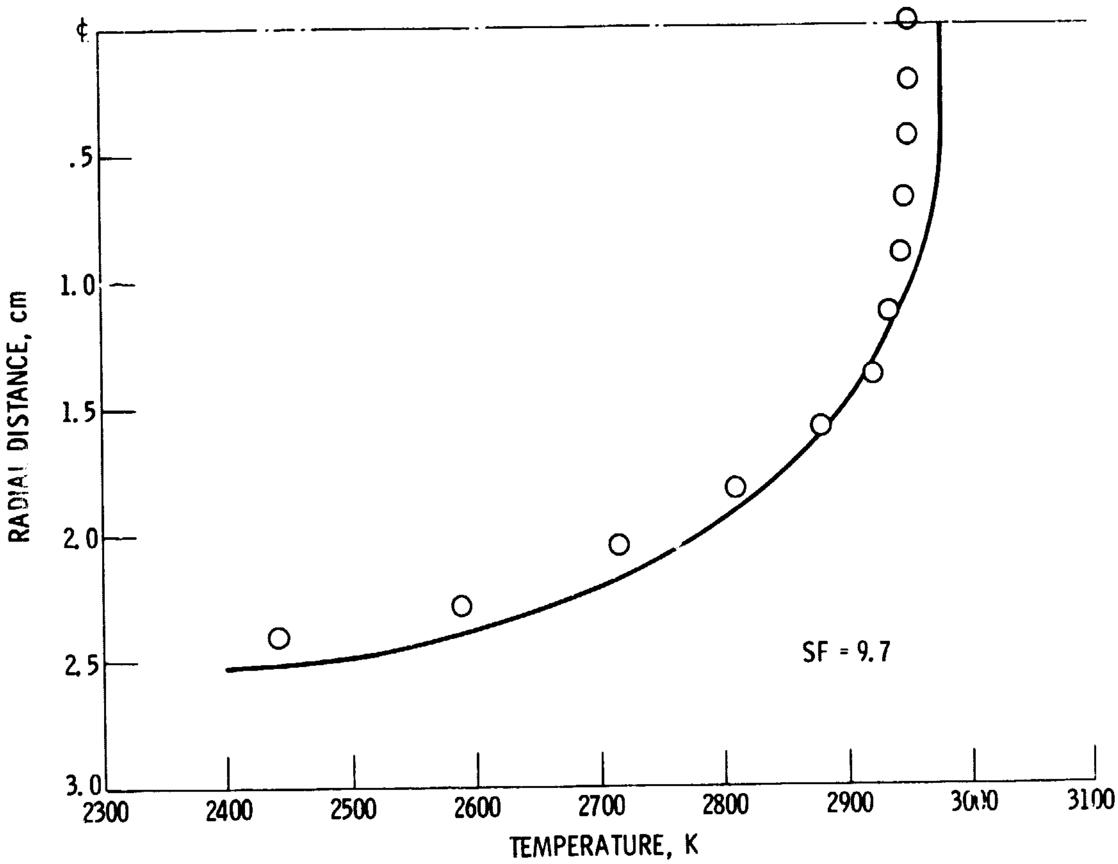

(c)

Figure 2. - Concluded.

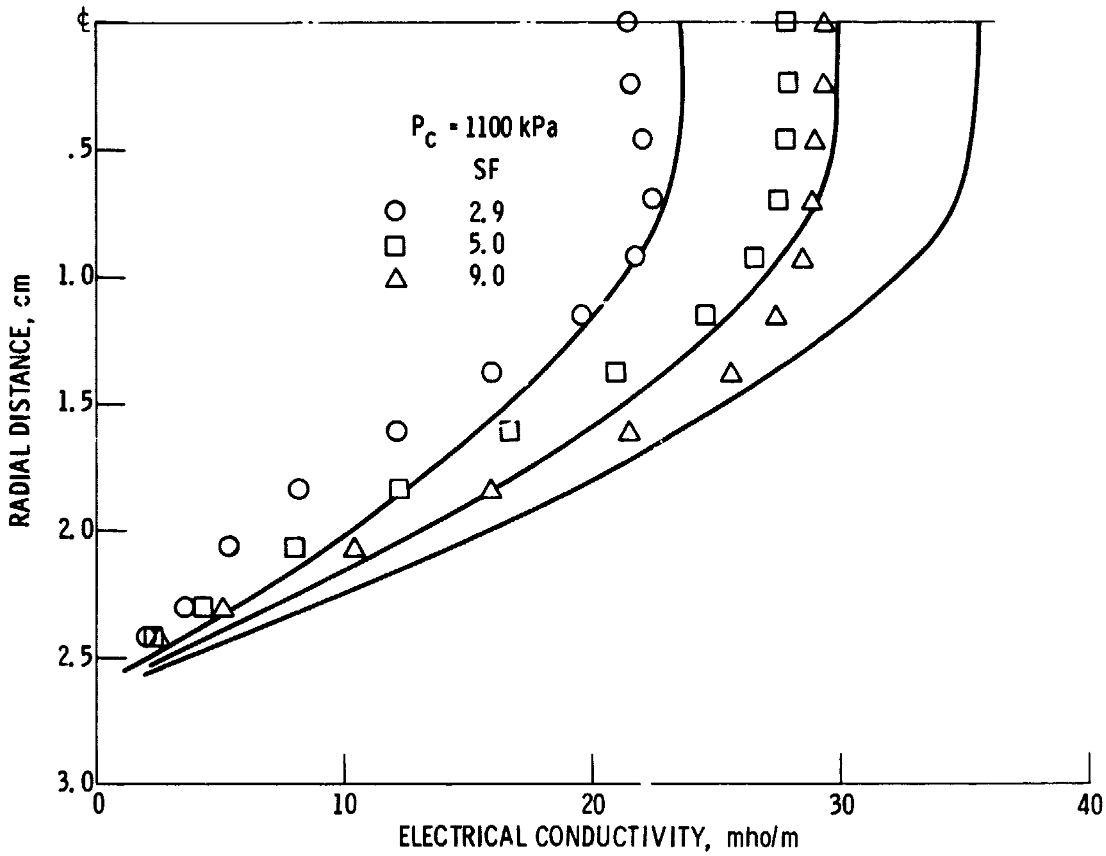

Figure 3. - Comparison with data for electrical conductivity profiles. The wall temperature equaled 600 K in the calculations.

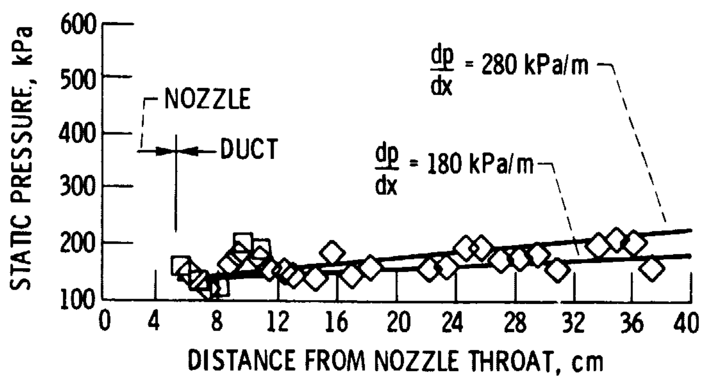

Figure 4. - Static pressure distribution data along the duct from [1] and the approximated pressure gradient lines.

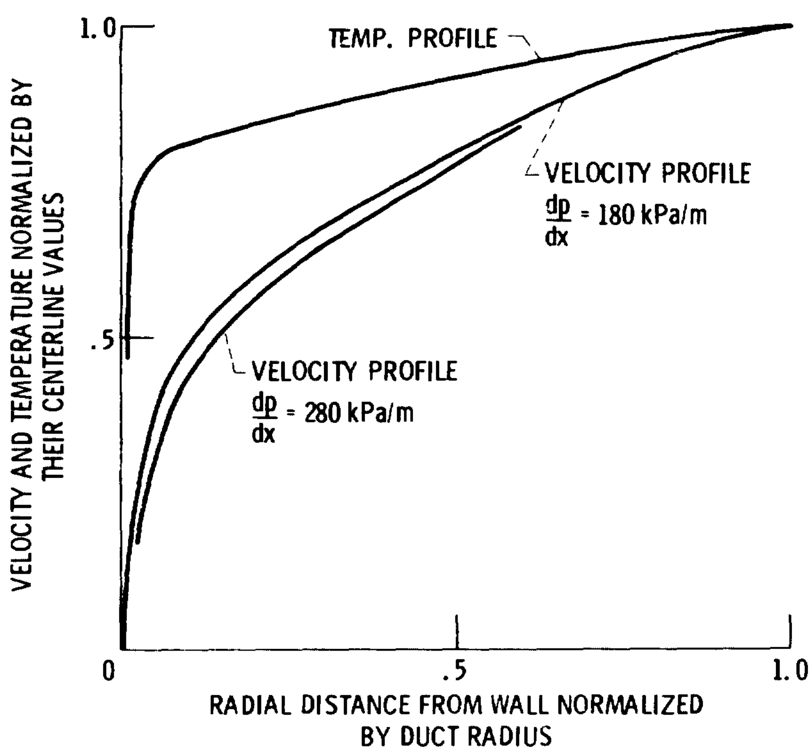

Figure 5. - Fully developed velocity and temperature profiles.

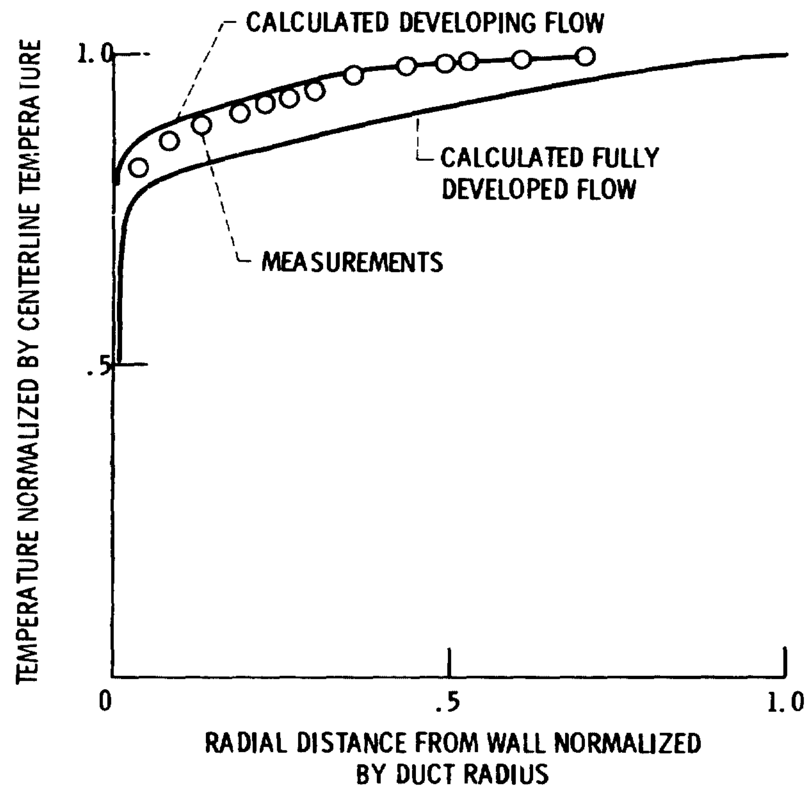

Figure 6. - Comparison of calculated temperature distributions with measured values.